DYNAMIC RESPONSE OF TAILINGS DAMS TO EARTHQUAKES

Jey K. Jeyapalan (I)
Presenting Author: Jey K. Jeyapalan

SUMMARY

Many mines use tailings dams built of coarser portion of tailings to impound the finer portion of tailings which are very wet. Because of the poor quality of construction and maintenance many of these dams were found to be extremely vulnerable to earthquake loads, and the existence of these potentially hazardous impoundments is of considerable concern to the public and to the mining industries. Although there are, however, several fundamental differences between the dynamic responses of tailings dams and water storage dams, many of these tailings dams are being designed using procedures developed for water retaining dams. The purpose of this paper is to indicate the effects of one of these differences on the dynamic response of tailings dams during and after an earthquake.

INTRODUCTION

Mine tailings are a waste byproduct of mining and milling operations. Because they have no commercial value, their disposal is often given little or no consideration. Most mines construct tailings dams by using the coarser portion of the tailings to impound the finer portion of the tailings. Also, many of these poorly constructed embankments have one or more of the following deficiencies; (1) extremely steep slopes, (2) no emergency outlet structures, (3) high water levels, and (4) cracks or sloughs in the embankments.

The performance of a tailings dam is greatly influenced by the method of construction. The upstream method of construction shown in Fig. 1 is the oldest and the most commonly used construction method. Usually all the tailings are discharged by spigotting in an upstream direction from the top of the dike. Separation of the coarse and fine portions occurs as the tailings flow into the pond, the coarser portions settling out first and forming a sand beach. The height of the embankment is raised either by dragging up sandy material from the beach or by the natural hydraulic deposition process. The main advantage of the upstream method is its simplicity and the resulting economy. The disadvantage of this type of construction is the inherent weakness due to the fact that the finer portion or slimes underlie higher portions of the dike. Also, little engineering planning or expertise is put into the design of these dams. Thus, many tailings dams built by this method have failed (Ref. 1), and the existence of these potentially hazardous impoundments is of considerable concern to the public and to the mining industries.

(I) Assistant Professor, Department of Civil Engineering, Texas A&M University, College Station, Texas, USA

BEHAVIOR OF TAILINGS UNDER SEISMIC LOADING

Mine tailings consist predominantly of sand and silt sizes, and it would be expected that their behavior under undrained conditions would be very similar to that of loose sand. Because the volume of a saturated sample of loose sand can not change during undrained loading, the contractive volume change tendency causes a large positive change in pore pressures. The shearing resistance decreases as a function of the stress ratio and the number of loading cycles. It has been shown (Ref. 2) that the behavior of tailings under cyclic loading to be very similar to the behavior of sands under cyclic loading. Ishiara (Ref. 2) showed that the resistance of tailing materials to liquefaction is dependent on the cyclic stress intensity and the relative density of the tailings deposit.

The reduced shear strength, for use in slope deformation calculations can be estimated using the cyclic pore pressure ratio, r_u (u_g/σ'_o) defined by Ref. (3) and Ref. (4) as follows:

$$\tau_R = \tau_s (1 - r_u) \qquad (1)$$

where $r_u = 2/\pi \text{ arc sin } (N/N_1)^{1/2\alpha}$

τ_s = static shear strength,

τ_R = residual shear strength,

N = number of significant stress cycles,

N_1 = number of stress cycles to cause initial liquefaction, and

α = 0.7 for most soils.

The above reduced shear strength will be used in the slope deformation analysis procedures presented in the next section. In order to be able to assess the consequences due to the unrestrained movement of such tailings slopes, it is necessary to develop analysis procedures that can be used for predicting the extent of slope movement. Such procedures will involve determining slope configurations that will satisfy force equilibrium and volume conservation. The details of such analysis procedures are given in the following section.

SIMPLIFIED ANALYSIS OF SLOPE DEFORMATION

In order to determine the stable configuration of the tailings slope after a shear strength reduction due to a design earthquake, a simplified slope stability analysis procedure which satisfies force equilibrium and volume conservation is required.

For this problem, in Ref. (5) a simple slope stability analysis procedure has been proposed which assumed plane strain conditions. In this analysis, the behavior of the tailings shortly after the earthquake is

assumed as undrained. In order to keep the analysis simple, homogeneous material properties are assumed throughout the slope, and only planar failure surfaces are considered in the evaluation of slope stability. During and shortly after an earthquake, due to the build-up of excess pore pressures, the shear strength of the tailings will decrease and the slope will deform to reach a stable configuration. In Ref. (6) it was shown that during movement the toe of the slope will assume approximately a parabolic shape and the stable height of the toe will be $4\tau_R/\gamma$. Due to the effect of lateral spreading of the tailings, the flowing debris will form a conical pile and therefore, the above plane strain analyses cannot be used to assess the extent of movement. In this paper, a conical mass will be analyzed in an axisymmetric stress condition.

The analysis will be developed by satisfying force equilibrium and volume conservation on a small segment of the slope, shown in Fig. 2, located on the most downstream portion of the slope. This segment of the conical slope is analyzed because it is the most critical in terms of stability. This portion of the slope will move the greatest distance if the slope is unstable. The analysis will be developed in two parts, as in the plane strain solution, as follows:

Case 1 The critical failure surface is inclined at an angle $\psi_c > \beta$, the bed slope.

The component of the driving force, F_D can be calculated for the mass above the failure surface as shown in Fig. 2 as

$$F_D = \gamma \sin \left[\frac{12\tau_R}{\gamma} + R(\tan \alpha - \tan \psi)\right] \frac{R^2}{6} d\theta \qquad (2)$$

where γ = total unit weight of tailings,

R = radius of conical segment,

ψ = angle of inclination of failure surface,

τ_R = reduced shear strength of tailings, and

α = tailings slope angle.

The shearing resistance, F_R can be evaluated for the sliding mass as

$$F_R = \tau_R \frac{R^2}{2} \sec \psi \, d\theta \qquad (3)$$

The flowing thickened tailings will assume a stable configuration when the driving and resisting forces are in equilibrium, or when

$$F_R = F_D \qquad (4)$$

Therefore from equations (1) and (2), and after some algebraic simplification,

$$\tau_R = \frac{\gamma R (\sin 2\psi \tan \alpha - 2 \sin^2 \psi)}{6 (1 - 2 \sin 2\psi)} \qquad (5)$$

For the critical failure plane,

$$\frac{d\tau_R}{d\psi} = 0 \tag{6}$$

and from eqs. (5) and (6) and after some algebraic simplification,

$$\psi_c = \tan^{-1} \left[\frac{\tan \alpha}{2 - \tan \alpha}\right] \tag{7}$$

From the geometry of the slope,

$$R = \left[H - \frac{4\tau_R}{\gamma}\right] \frac{1}{(\tan \alpha - \tan \beta)} \tag{8}$$

where β = bed slope, and

H = height of the slope

Using eqs. (7) and (8) in eq. (5) gives

$$N_s = 4 + \frac{6\,(1 - 2 \sin 2\psi)(\tan \alpha - \tan\beta)}{(\sin 2\psi \tan \alpha - 2 \sin^2\psi)} \tag{9}$$

where $N_s = \frac{\gamma H}{\tau_R}$, the slope stability number

Case 2 The critical failure surface is inclined at an angle $\psi_c < \beta$.

For this case, as in the plane strain solution, the failure plane will be inclined at

$$\psi_c = \beta \tag{10}$$

The slope stability number, N_s, can be calculated using eq. (10) in eq. (9).

The above stability analysis can be best presented in a dimensionless chart, shown in Fig. 3.

To complete the analysis, the volume conservation requirement must be satisfied. As in the plane strain solution given in Ref. (5), an approach similar to that of Ref. (7) will be used. The volume, V, of the thickened tailings contributing to the movement is given by

$$V = \left[\frac{12\,\tau_R}{\gamma} + R\,(\tan \alpha - \tan \beta)\right] \frac{R^2}{6}\, d\theta \tag{11}$$

Using eq. (8) in eq. (11) and rearranging yields

$$\frac{6V}{H^3} = \frac{(1 - 48/N_s^2 + 128/N_s^3)\, d\theta}{(\tan \alpha - \tan \beta)^2} \tag{12}$$

If a fraction, f, of the original deposit is included in the flow slide of the tailings,

$$V = \frac{fH_o^3 \, d\theta}{6 \, (\tan \alpha_o - \tan \beta)^2} \tag{13}$$

And using eq. (13) into eq. (12) yields

$$\frac{fH_o^3 \, d\theta}{H^3 \, (\tan \alpha_o - \tan \beta)^2} = \frac{(1 - 48/N_s^2 + 128/N_s^3) \, d\theta}{(\tan \alpha - \tan \beta)^2} \tag{14}$$

which can be rewritten as

$$N_v = \frac{(1 - 48/N_s^2 + 128/N_s^3)}{(\tan \alpha - \tan \beta)^2} \tag{15}$$

where $$N_v = \frac{fH_o^3}{H^3 \, (\tan \alpha_o - \tan \beta)^2}$$, the dimensionless volume (16)

in which f = fraction of the original tailings involved in the flow slide,

H_o = original tailings slope height,

α_o = original tailings slope angle, and

H = height of tailings during the flow.

Values of eq. (15) are presented in Fig. 4. The solution procedure for conical geometry is similar to that for the plane strain solution given in Ref. 5.

The values of H and α defining the stable configuration of the tailings undergoing movement are determined using Figs. 3 and 4 as follows:

Step 1: For known values of γ, H_o, α_o, τ_R, β, and f, calculate N_v and N_s by assuming H and α.

Step 2: Use Figs. 3 and 4 to arrive at a value for N_s consistent with that calculated in Step 1.

Step 3: Repeat Steps 1 and 2 until the results converge.

CONCLUSIONS

The following conclusions can be drawn from this paper:

1. The tailings dams are more vulnerable to earthquake induced failures in comparison to water storage dams.

2. When a breach occurs at a tailings dam, the waste materials spread in the form of a partial cone, downstream of the breach. Therefore it is necessary to predict the potential run-out distances as part of the design calculations.

3. The procedure outlined in this paper will yield a lower bound estimate of the run-out distance, due to the fact that inertial and viscous forces are ignored in these analyses.

REFERENCES

1. Jeyapalan, J. K. (1981), "Flow Failures of Some Mine Tailings Dams," Geotechnical Engineering, Vol. 14, No. 2, December, pp. 153-166.

2. Ishihara, K., Troncoso, J., Kaware, Y., and Takahashi, Y. (1980), "Cyclic Strength Characteristics of Tailings Materials," Soils and Foundations, Vol. 20, No. 4, December.

3. Seed, H. B., and Idriss, I. M. (1981), "Evaluation of Liquefaction Potential of Sand Deposits Based on Observations of Performance in Previous Earthquakes," Preprint from the ASCE Technical Session No. 24 of the Fall National Convention, St. Louis, October.

4. Klohn, E. J., Maartman, C. H., Lo, R. C. Y., and Finn, W. D. L. (1978), "Simplified Seismic Analysis for Tailings Dams," ASCE Specialty Conference on Earthquake Engineering and Soil Dynamics, Pasadena, California, pp. 540-556.

5. Jeyapalan, J. K. (1982), "Earthquake Induced Movements of Thickened Tailings Slopes," Preprint of ASCE Technical Session on Dynamic Stability of Tailings Dams, Fall National Convention, New Orleans, Louisiana, October.

6. Jeyapalan, J. K. (1980), "Analyses of Flow Failures of Mine Tailings Impoundments," Ph.D. dissertation submitted to the University of California at Berkeley, August.

7. Lucia, P. C. (1981), "Review of Experiences with Flow Failures of Tailings Dams," Ph.D. Dissertation in Civil Engineering, University of California, Berkeley, December.

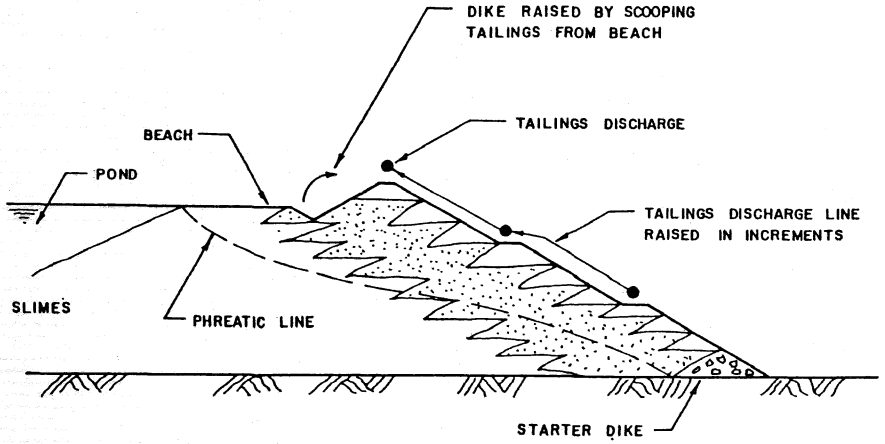

FIG. 1 - A TAILINGS DAM CONSTRUCTED USING CONVENTIONAL UPSTREAM METHOD

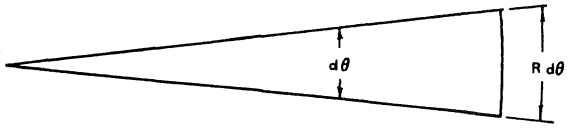

FIG.2 (a) - PLAN OF CONE SEGMENT

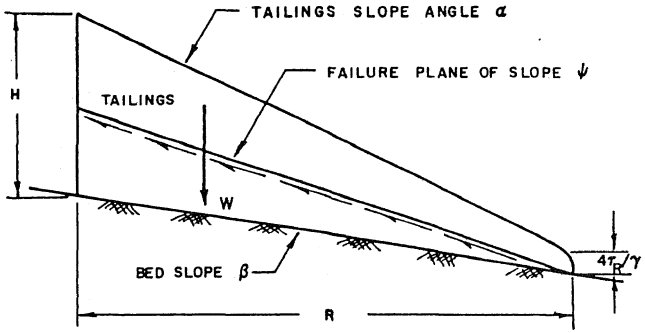

FIG.2 (b) - CROSS SECTION OF CONE SEGMENT

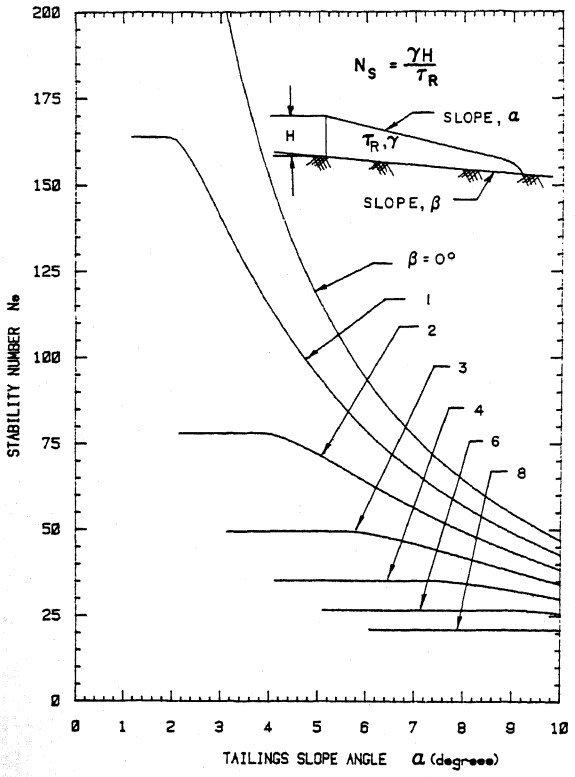

FIG. 3 - CONICAL SLOPE DEFORMATION CHART

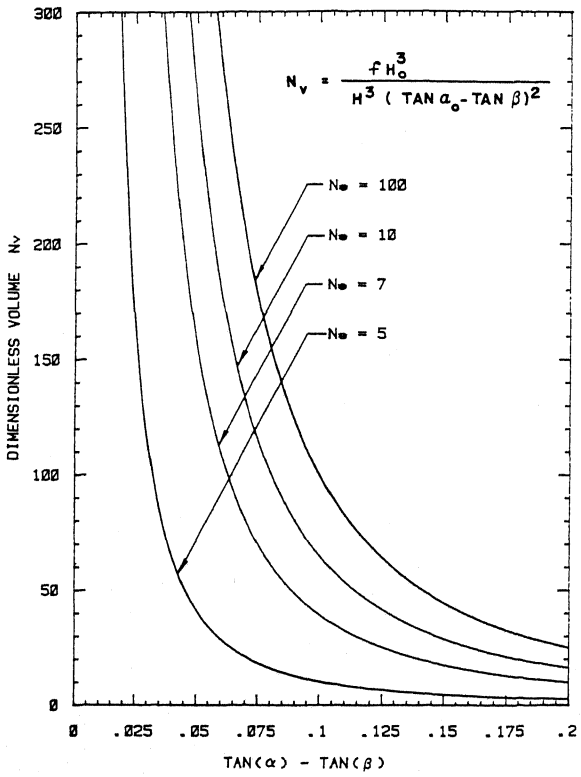

FIG. 4 - CONICAL VOLUME CHART